Optical and tribological properties of decorative titanium carbonitride coatings

L. Milschi, I. Belahsen, G. C. Lain, S. S. Tomiello, C. D. Boeira, L. T. Bim, F. Cemin, C. M. Menezes, B. L. Perotti, J. Catafesta & C. A. Figueroa

Published online: 26 Oct 2017.

Submit your article to this journal ↗

View related articles ↗

View Crossmark data ↗

Optical and tribological properties of decorative titanium carbonitride coatings

L. Milschi[a], I. Belahsen[a,c], G. C. Lain[b], S. S. Tomiello[a,b], C. D. Boeira[a], L. T. Bim[a], F. Cemin[a], C. M. Menezes[a], B. L. Perotti[a], J. Catafesta[a] and C. A. Figueroa[a,b]

[a]PGMAT – Universidade de Caxias do Sul, Caxias do Sul, Rio Grande do Sul, Brazil; [b]Plasmar Tecnologia Ltda., Caxias do Sul, Rio Grande do Sul, Brazil; [c]Ecole Européenne d'Ingénieurs en Génie des Matériaux, Nancy, France

ABSTRACT

Stainless steel and chromium-electroplated metal can change their metallic surface aspects into different colours by thin film deposition technologies. In this study, the colour change of titanium carbonitride (TiC_xN_y) thin films as a function of N_2 and CH_4 flow rates in the deposition process was investigated. TiC_xN_y thin films were deposited by cathodic arc in an industrial equipment at low temperature (125°C) for decorative purposes. The samples were analysed by X-ray diffraction, scanning electron microscopy, glow discharge optical emissions spectroscopy, nanohardness, nanoscratch test and colorimetric analysis. The colour slightly changes from yellow gold to light bronze with carbon addition in the thin film structure. Scratch test determines an increase of the critical load for both plastic deformation and delamination as the carbon content increases. The failure mode shifts from brittle/ductile mode to ductile mode with the increase of the carbon content.

Introduction

Thin films for decorative purposes can be deposited by many techniques such as plasma enhanced chemical vapour deposition and physical plasma deposition (PVD) [1,2]. Cathodic arc deposition (CAE-PVD) is appreciated due to its characteristics like high deposition rate, good adhesion, flexibility of deposition parameters, compatibility with many substrates and colour reproducibility [3–5]. Titanium nitride (TiN) and titanium carbide (TiC) coatings deposited by CAE-PVD combine good mechanical properties and chemical stability [6–9] with appreciated yellow gold and dark grey colour to decorative purposes. Another feature of CAE-PVD is the possibility to produce ternary thin films, which offer interesting properties for decorative applications [3]. A wide range of colours and different mechanical, tribological and/or optical properties can be obtained from these hard films depending on the phases that make part of the material.

Titanium carbonitride (TiC_xN_y) is a ternary compound that combines the chemical resistance of the TiN and good wear protection of the TiC [10]. In addition, TiC_xN_y thin films provide a large colour range, which starts in yellow gold colour for TiN to dark bronze for TiC [3,8], including a variety of hues with subtle difference. This is important to decorative purposes where minimal colour difference might be required. The properties and colours depend on the stoichiometry of thin films, technique and temperature used during the deposition process. Moreover, mechanical and tribological properties must be controlled in order to guarantee high scratching resistance and high adhesion on metallic substrates.

In this context, the goal of this work is to produce TiC_xN_y thin films with subtle colour differences by CAE-PVD technique and characterise its structural, mechanical and tribological properties. The colour variation control was achieved by changing the flow rate of nitrogen and methane gases in the deposition process at low temperature.

Experimental

The thin films were deposited on AISI 304 steel substrates ($20 \times 20 \times 0.5$ mm) previously polished until 3 μm with synthetic diamond paste, cleaned with alkaline rinse and washed ultrasonically with deionised water. A cathodic arc industrial equipment, developed by Guangdong Zhonghuan Vacuum Equipment Co. Ltd., with 12 Ti targets (diameter of 80 mm each) and equipped with a sample rotation system was used for the experiments. The chamber was pumped up to a base pressure of 2×10^{-2} Pa. After that, an etching process with Ar flux of 300 sccm, pressure of 10 Pa, bias voltage of 1100 V during 300 s was done. The titanium interlayers were deposited to improve the thin film adhesion [11] on substrates with bias voltage of 300 V, Ar flux of 1000 sccm at pressure of 2 Pa during 45 s. Finally, the TiC_xN_y thin film deposition process

Table 1. N_2 and CH_4 flow rates for TiC_xN_y thin film depositions.

Sample	CH_4 flux (sccm)	N_2 flux (sccm)	CH_4/N_2 flux ratio
TiC_xN_y (1:12)	50	600	1:12
TiC_xN_y (1:7)	70	500	1:7
TiC_xN_y (1:5)	90	440	1:5
TiC_xN_y (1:4)	110	400	1:4
TiC_xN_y (1:3)	130	400	1:3

was carried out with bias tension of 100 V and pressure of 6×10^{-1} Pa feeding with N_2 and CH_4 during 120 s. Table 1 shows the N_2 and CH_4 fluxes used during the TiC_xN_y thin film deposition. The temperature was maintained at 125°C during the deposition process.

A Shimadzu XRD-6000 diffractometer was used for X-ray diffraction in the crystalline phase and micro-structural characterisation. The operating conditions were as follows: Cu radiation ($\lambda = 1.5418$ Å), 40 kV and 30 mA and 2θ rotation. The samples were rotated during the analysis in order to avoid the preferential orientation effects. The range of diffraction angles was 30−80° and the scanning speed was 2° per minute. Scanning electron microscopy (SEM) was carried out for morphology and microstructural analysis by using a Super Scan SSX-550 Shimadzu. Glow discharge optical emission spectroscopy (GD-OES) was used for in-depth chemical profiling analysis by using a GD-Profiler 2 – Horiba Scientific apparatus, operated at 20 W.

The sample colour was measured in triplicate using a Colorimeter Minolta (CM2500d) spectrophotometer with D65 and 10° of viewing angle, represented by Cie-Lab colour space according to Ref. [7].

Mechanical and nanotribological characterisations were performed with a NanoTest-600 MicroMaterials Ltd. equipment. A three-sided Berkovich pyramidal diamond tip was used for the hardness measurements. The load speed was 0.01 mN s^{-1}, applied from 0.01 mN and the load was applied at a depth of 30 nm in order to avoid the substrate influence. For adhesion measurements, nanoscratch tests were done using a conical diamond tip with 25 µm of radius and a load speed of 0.01 mN s^{-1}, applied from 0.01 to 470 mN. A Zeiss AxioScope optical microscope (500×) was used to examine the worn tracks.

Results and discussion

Crystalline structure, microstructural, morphological and chemical characterisation

Figure 1 shows the XRD patterns of as-deposited TiC_xN_y thin films at different N_2:CH_4 compositions. Such a compound shows a cubic structure and space group symmetry fm-3m for all the samples according to the JCPDS card 42-1489. The peaks at 2θ−36.35°, 42.45° and 61.62° correspond to (111), (200) and (220) TiC_xN_y crystallographic planes, respectively. The vertical dashed lines represent the (111), (200) and (220) crystallographic planes for a representative
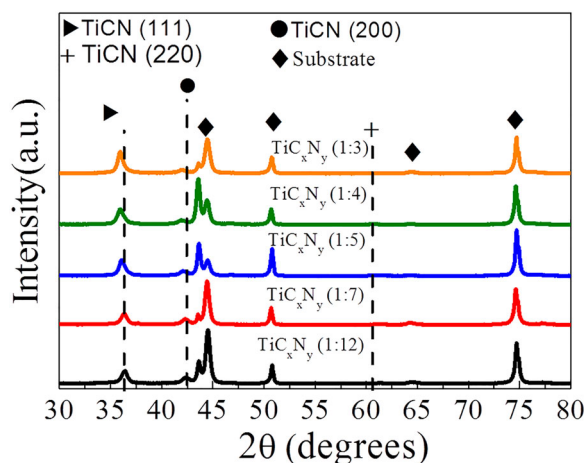
Figure 1. X-ray diffraction patterns for the TiC_xN_y thin films.

$TiC_{0.3}N_{0.7}$ compound. One can observe that a slight shift of (111), (200) and (220) planes towards to lower diffraction angles are followed by a higher carbon concentration in the gas mixture during the deposition process.

Titanium carbonitride structures are described in many works as a solid solution of TiC and TiN phases [12–15]. That is because the diffraction peaks of TiC, TiN and TiCN are near and, consequently, they are hard to be distinguished by XRD [8,14,16]. The quantification of crystalline phases that constitute this solid solution can be estimated by application of the Vegard's law [14,17]. The lattice parameter and TiC_xN_y composition relationship is shown in Figure 2. The increase of the lattice parameter, which is associated with the shift of the TiC_xN_y crystallographic planes, suggests an isotropic deformation through expansion as the carbon concentration increases because the carbon atom is slightly larger than nitrogen [12]. This expansion can also be associated with the atoms organisation according to the Levi's model (II) [13]. The atom mobility in the deposited thin film cells decreases with carbon addition [12].
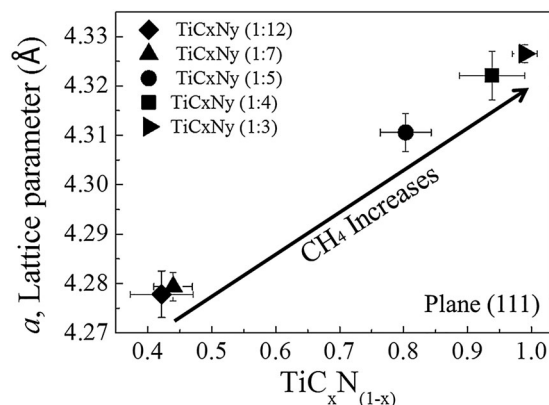
Figure 2. Experimental lattice parameter and TiC_xN_y composition relationship according to Vegard's law for (111) crystallographic plane.
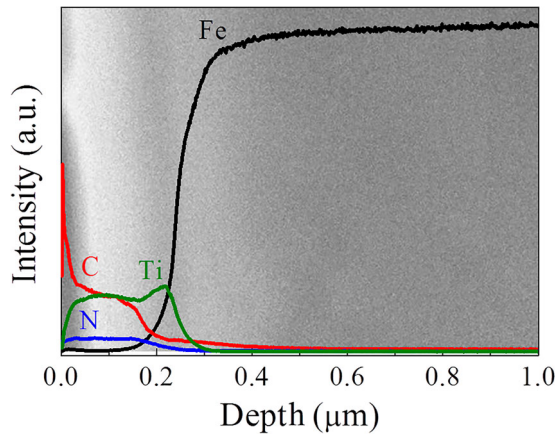
Figure 3. SEM image in cross-section of the TiC_xN_y thin film obtained with 1:4 flux ratio where the chemical profile obtained by GD-OES is superimposed.
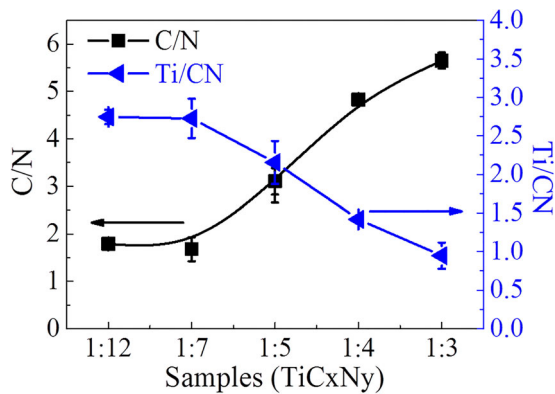

Figure 4. C/N and Ti/CN signal intensity ratios obtained by GD-OES as a function of flux ratio.

Figure 3 shows the cross-section SEM image of the TiC_xN_y(1:4) sample. For completeness, the relative chemical profile of such a sample obtained by GD-OES is superimposed on the image. One can see that the material system is constituted by an outermost layer of TiC_xN_y thin film followed by a titanium interlayer Ti, and, finally, the AISI 304 substrate emerges. The polycrystalline morphology, as defined in the temperature and pressure zones by the Thornton diagram, is adopted for our TiC_xN_y thin film. Moreover, the Schneider et al. [12] work claims that the increase

of carbon in the structure decreases the adatom mobility and, hence, the columnar structuration.

The thickness of titanium carbonitride thin films was estimated by the SEM images ranging from 100 to 150 nm. By using the thickness of TiC_xN_y thin films measured directly by SEM, the chemical profiles obtained by GD-OES could be calibrated in length units. Thus, the Ti interlayer thickness is ~50 nm in all the samples.

The C/N and Ti/CN signal ratios obtained by GD-OES analysis are shown in Figure 4. The C/N ratio increases with the increase of CH_4 addition in the gas mixture during the deposition process while the Ti/CN ratio decreases [1,18]. Therefore, one can conclude that the methane addition leads to increase the carbon content in the samples. This effect will enable us to explain the colour variation in the next section.

Colour characterisation

The visual aspect of the samples is shown in Figure 5. The colour changes from a slightly gold to bronze as the carbon content increases [5,19]. Although the colour difference was subtle, the decorative purpose appreciates such detail.

The CieLab system was used to quantify colour differences among samples [20,21]. This system was developed by the *Comission Internationale l'Éclairage* (CIE) and it is used to characterise colours in terms of a*, b* and L*, where a* axis represents red/green colours, b* axis represents yellow/blue colours and L* represents the lightness. Figure 6(a) shows a* and b* and 6 (b) shows L* as a function of the N_2 and CH_4 in the gas mixture for deposition of TiC_xN_y samples. The L* reduction shown in Figure 6(b) is expected because, as the carbon content increases, the proportion of carbon in the TiC_xN_y phase also increases, reducing the lightness [5,8]. The partial lightness can be attributed to Ti atoms, which contribute to metallic brightness [1,18].

The chromaticity (C_{ab}*) and tonality (h_{ab}*) indexes as function of the carbon content in the gas mixture are shown in Figure 7. The chromaticity tends to decrease as the carbon content increases and the TiC_xN_y thin
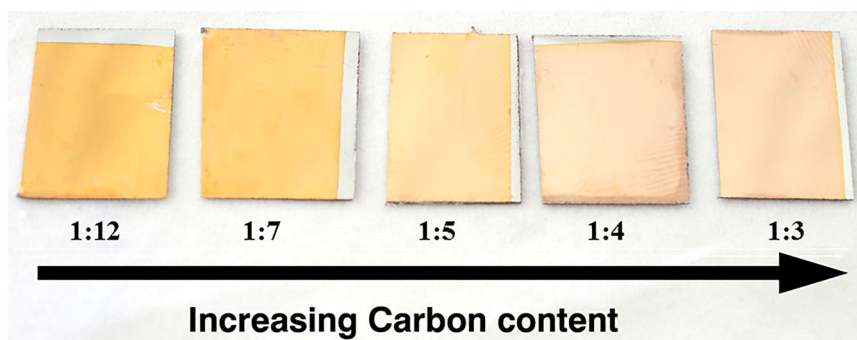

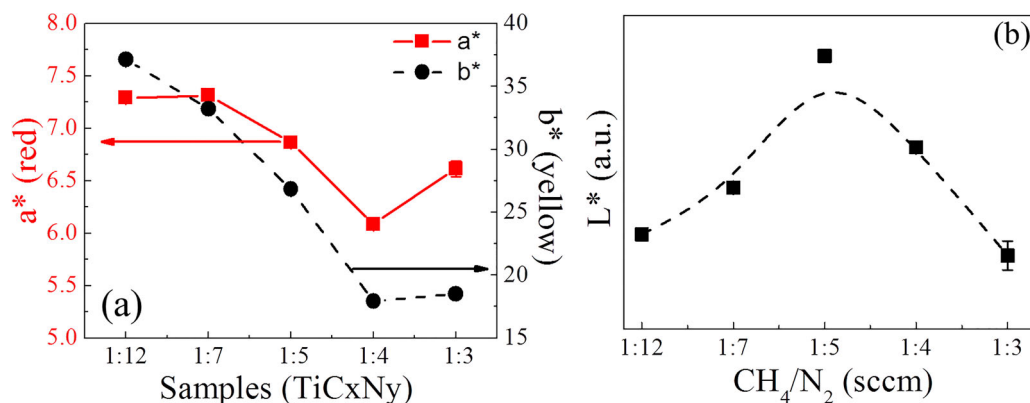**Figure 5.** TiC_xN_y colour changing with the increasing of the carbon in the gas mixture.

Figure 6. (a) Colour variation based on a* and b*, where a* represents the red colour and b* represents the yellow colour. (b) Lightness variation. In both figures, the variation is in function of the N_2 and CH_4 fluxes in the gas mixture.

film becomes more opaque. This result is due to the loss of free electrons according to Drude's theory [18,22].

A colour-difference calculation was made to quantify the colour variation among samples [20,21]. The ΔE^*, according to the CIE, represents the difference between two colours and can be estimated by $\Delta E^* = E_2^* E_1^* = (L_2^* - L_1^*)^2 + (a_2^* - a_1^*)^2 + (b_2^* - b_1^*)^2$, where the indexes 1 and 2 denote two different colours. Figure 8 shows the ΔE^* where the x axis represents the difference between two samples.

Mechanical and tribological properties

The mechanical properties are important for decorative thin films because they may improve the scratch resistance and ensure surface integrity.

Nanohardness results for the TiC_xN_y thin film are shown in Figure 9. The values were obtained for a final depth of 30 nm in order to avoid the substrate influence. One can see that the hardness slightly decreases with the increase of the carbon content. The hardness measurements are relatively low when compared with other studies, where the TiC_xN_y thin films were deposited at higher temperatures than those reported here and by different deposition techniques, generally, for functional applications (cutting

tools) [23]. However, these values are acceptable for decorative purpose because they are usually not submitted to aggressive wear regimes.

The ratio between hardness and elastic modulus (H/E), where the elastic modulus was obtained from Oliver and Pharr method [24] ($\nu = 0.18$), and the relation between hardness and the elastic modulus (E), H^3/E^2, can be used as an indicator of elastic and plastic
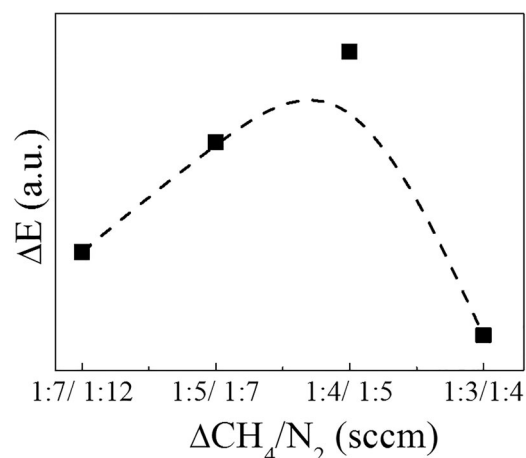

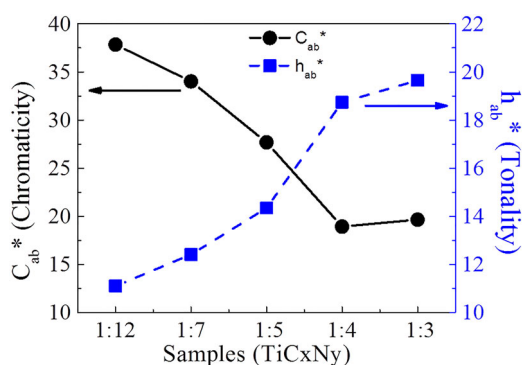**Figure 8.** Colour difference between two colours.

Figure 7. Chromaticity and tonality as function of the N_2 and CH_4 fluxes in the gas mixture.
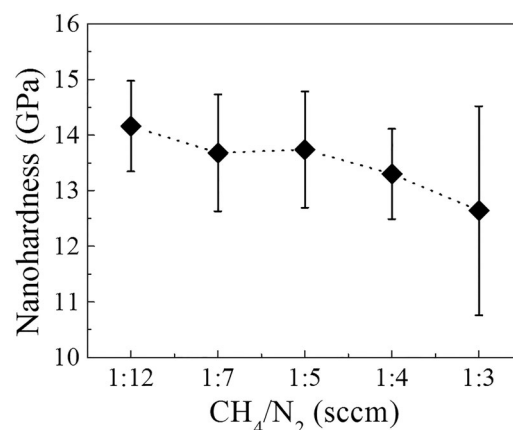

Figure 9. Nanohardness of TiC_xN_y thin films as a function of the carbon content in the gas mixture.
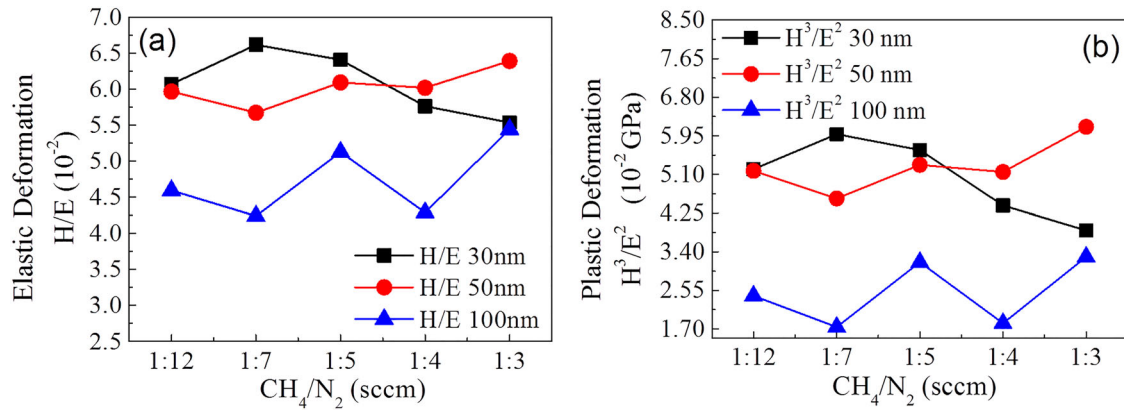
Figure 10. (a) *H/E* and (b) H^3/E^2 ratios as a function of the N_2 and CH_4 fluxes in the gas mixture at three different depths.

deformation, respectively [25]. The evolution of *H/E* and H^3/E^2 is shown in Figure 10(a,b), respectively, at three different indentation depth. In both cases, higher ratio values imply higher scratch resistance. It is important to remark that the results obtained at 100 nm are influenced for the mechanical properties of the substrate.

The scratch resistance is mostly a measure of plastic deformation mechanisms and adhesion forces between the deposited thin film (layer and interlayer) and the substrate. Both critical loads to induce plastic deformation (Lc1) and delamination (Lc2) were estimated by using optical micrograph and the loads applied in the scratch test. Figure 11 shows both Lc1 and Lc2 as a function of the carbon content in the gas mixture. One can see that Lc2 increases with the increase of the carbon content in the gas mixture. As published elsewhere [23], hardness decreases slightly as the TiC$_x$-N$_y$ thin film becomes more ductile and, also, the crack propagation energy increases with the increase of the carbon content, which is in agreement with our results.

Figure 12 shows the failure behaviour at increasing carbon content from the left to the right. One can see that the failure mechanism changes as the carbon content increases. The recovery and buckle spallation failure modes are observed in samples 1:12 and 1:7 (CH$_4$/

N_2 sccm), which are characteristics of the compressive stress and brittle-ductile behaviour in the TiC$_x$N$_y$ thin films. This kind of failure is a response to the compressive stress induced by the moving tip where crack occurs in high-stress regions [26,27]. In samples 1:4
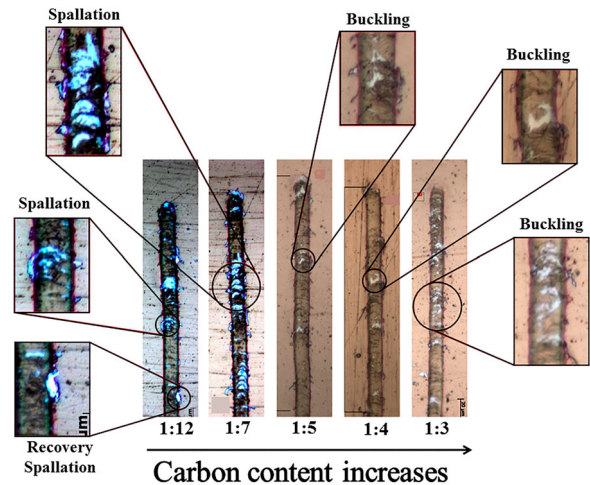

Figure 12. Failure modes after scratch test as a function of the carbon content in the gas mixture. A is spallation, B is recovery spallation, and C is buckle spallation failure mode.
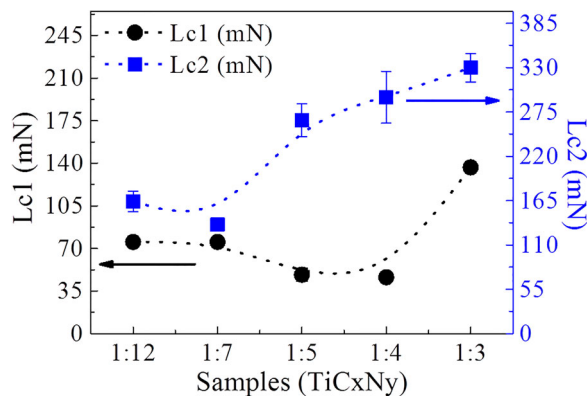

Figure 11. Lc1 and Lc2 as a function of the N_2 and CH_4 fluxes in the gas mixture.
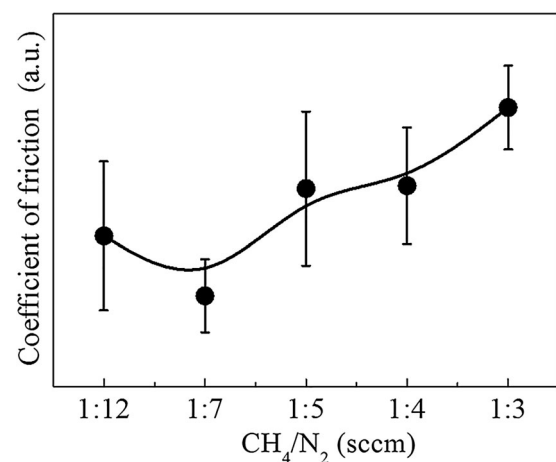

Figure 13. Coefficient of friction of TiC$_x$N$_y$ thin films as a function of the carbon content in the gas mixture.

and 1:3 (CH_4/N_2 sccm), the buckling fracture mode is more representative. This mode is expected in ductile thin films [11].

Finally, the friction coefficient (COF) is shown in Figure 13. One can see that the COF increases as the carbon content increases. This is due to the fact that thin films become softer, as seen in Figure 9, which increases the contact area during sliding and, thus, the total friction force.

Conclusions

The microstructural, chemical, mechanical, tribological and optical properties of TiC_xN_y thin films, deposited at low temperature, were analysed at different carbon contents. The TiC_xN_y thin films that contain the highest carbon content in the structure showed the lowest hardness. A lower hardness implies a higher ductility, as observed in the failure mode. As the carbon content increases, the scratch resistance and delamination increase as well. By varying the carbon content, it was also possible to achieve a range of colours from yellow gold to light bronze. The results of this work can be used in the industrial production of thin films for decorative applications, at low temperatures, with different colours and good enough scratch resistance.

Disclosure statement

No potential conflict of interest was reported by the authors.

References

[1] Jedzejowski P, Klemberg-Spieha JE, Matinu L. Optical properties and color of hard quaternary nanocomposite $TiC_xN_y/SiCN$ coatings prepared by plasma enhanced chemical vapor deposition. Surf Coat Technol. 2004;188–189:371–375.

[2] Reiners G, Hantsche H, Jehn HA, et al. Decorative properties and chemical composition of hard coatings. Surf Coat Technol. 1992;54–55:273–278.

[3] Skoworonsky L, Wachowiak AA, Grabowski A. Characterization of optical and microstructural properties of semitransparent $TiO_2/Ti/glass$ interference decorative coatings hard coating for decorative applications. Appl Surf Sci. 2016;388:731–740.

[4] Carvalho P, Borges J, Rodrigues M.S, et al. Optical properties of zirconium oxynitride films: The effect of composition, electronic and crystalline structures. Appl Surf Sci. 2015;358:660–669.

[5] Damond E, Jacquot P, Pagny J. TiC_xN_{1-x} coatings by using the arc evaporation technique. Mater Sci Eng: A. 1991;140:838–841.

[6] Devia DM, Restrepo-Parra E, Arango PJ. Comparative study of titanium carbide and nitride coatings grow by cathodic vacuum arc technique. Appl Surf Sci. 2011;258:1164–1174.

[7] Chappé JM, Fernandes AC, Cunha L, et al. TiN-based decorative coatings: color change by addition C and O. J Optoelectron Adv Mater. 2008;10(4):900–903.

[8] Moura C, Cunha L, Chappé JM, et al. Study of thermal stability of Ti(C, O, N) decorative coatings. Plasma Process Polym. 2009;6:S755–S759.

[9] Lain GC, Cemin F, Menezes CM, et al. Bias influence on titanium interlayer for titanium nitride films. Surf Eng. 2016;32:279–283.

[10] Mütinsterer S, Kohlhof K. Cavitation protection by low temperature TiCN coatings. Surf Coat Technol. 1995;74–75:642–647.

[11] Bull SJ. Failure modes in scratch adhesion testing. Surf Coat Technol. 1991;50:25–32.

[12] Schneider JM, Voevodin A, Rebholz C, et al. X-Ray diffraction investigations of magnetron sputtered TiCN coatings. Surf Coat Technol. 1995;74–75:312–319.

[13] Levi G, Kaplan WD, Bamberger M. Structure refinement of titanium carbonitride (TiCN). Mater Lett. 1998;35:344–350.

[14] Ospina-Ospina R, Jurado JF, Vélez JM, et al. Structural and morphological characterization WC_xN_y thin films grown by pulsed vacuum arc discharge in an argon–nitrogen atmosphere. Surf Coat Technol. 2010;205:2191–2196.

[15] Shan L, Wang Y, Li J, et al. Tribological behaviours of PVD TiN and TiCN coatings in artificial seawater. Surf Coat Technol. 2013;226:40–50.

[16] Cheng YH, Browne T, Heckerman B, et al. Influence of the C content on the mechanical and tribological properties of the TiCN coatings deposited by LAFAD technique. Surf Coat Technol. 2011;205:4024–4029.

[17] Jacob KT, Raj S, Rannesh L. Vegard's law: a fundamental relation or an approximation? Int J Mater Res. 2007;98:776–779.

[18] Alves LA, Sagás JC, Damião AJ, et al. Drude's model optical parameters and the color of TiN_x films obtained through reflectivity measurements. Braz J Phys. 2015;45:59–63.

[19] Beck U, Reiners G, Urban I, et al. Evaluation of optical properties of decorative coatings by spectroscopic ellipsometry. Thin Solid Films. 1992;220:234–240.

[20] Konica Minolta, INC. Precise Color Communication, Color Control for Perception for Instrumentation. Booklet for download from Konica Minolta, INC web site. 2007.

[21] Fairchild MD. Color appearance models. 2ª. Rochester: John Wiley and Sons, Ltd.; 2005. ISBN 0-470-01216-1.

[22] Fuentes GG, Elizalde E, Sanz JM. Optical and electronic properties of TiC_xN_y films. J Appl Phys. 2001;90:2737–2743.

[23] Sun Y, Lu C, Yu H, et al. Nanomechanical properties of TiCN and TiCN/Ti coatings on Ti prepared by filtered Arc depositions. Mater Sci Eng: A. 2015;625:56–64.

[24] Oliver WC, Pharr GM. An improved technique for determining hardness and elastic modulus using load

and displacement sensing indentation experiments. J Mater Res. 1992;7:1564–1583.

[25] Musil J, Jirout M. Toughness of hard nanostructures ceramic thin films. Surf Coat Technol. 2007;201:5148–5152.

[26] Bull SJ. Failure mode maps in the thin films scratch adhesion test. Tribol Int. 1997;30:491–498.

[27] Bull SJ, Berasetegui EG. An overview of the potential of quantitative coating adhesion measurement by scratch testing. Tribol Int. 2006;39:99–114.